ISBN: 978-3-95450-233-2 ISSN: 2673-5504 doi:10.18429/JACoW-SRF2021-SUPCAV009

FIRST Nb_3Sn COATING AND CAVITY PERFORMANCE RESULT AT KEK

K. Takahashi*, Sokendai, Ibaraki, Japan
H. Ito, E. Kako, T. Konomi, T. Okada, H. Sakai, K. Umemori, KEK, Ibaraki, Japan

Abstract

At the High Energy Accelerator Research Organization (KEK), Nb_3Sn vapor diffusion R&D for high-Q performance has just commenced. A coating system via vapor diffusion was constructed, and the samples were coated using the system. The cavity-coating parameters were determined based on the results of the evaluated sample. A TESLA-like single-cell cavity was applied to coat the Nb_3Sn film, and its performance was evaluated by a vertical test. In this paper, we report on the cavity coating process and the result of cavity performance test.

INTRODUCTION

Nb_3Sn cavities have a high Q-value at a temperature of 4.2 K, which is almost equal to that of Nb cavity at 2 K; cryocoolers can be used to achieve the operating temperature of 4.2 K. Therefore, a small superconducting radio frequency (SRF) accelerator using a Nb_3Sn cavity is expected to be applied in various fields, such as RI production and water purification. Nb_3Sn vapor diffusion R&D for high-Q has just started at KEK, where Nb_3Sn films were coated on Nb substrates using the constructed coating system.

COATING SYSTEM

At KEK, a Nb_3Sn coating system via vapor diffusion was constructed [1]. It is a vertical-type coating system capable of coating a 1.3 GHz 3-cell cavity. Tin and tin chloride crucibles were used for the sample and cavity coating. Both crucibles were made of tungsten. A sample holder made of Nb was used for the sample coating. Figure 1 shows the coating parameters.

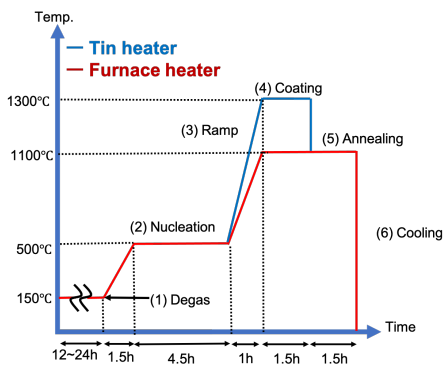

Figure 1: A typical coating process at KEK.

The coating process at KEK comprises a nucleation process, coating process, and annealing process, similar to that at Cornell University [2]. All nucleation processes described in this paper were performed at 500 °C for 4.5 h.

SAMPLE COATING

The coating parameters for the cavity were determined using samples: Two types of Nb substrates, Nb plates, and Nb foils, were used for the coating experiments. The Nb plates were cavity-grade Nb with a size of 7 mm × 7 mm and a thickness of 2.7 mm. The Nb plates were used to observe the surface condition. The Nb foil size was 4 mm × 50 mm with a thickness of 0.1 mm, and its RRR was approximately 30. The Nb foils were used to evaluate the Nb_3Sn film thickness and transition temperature (T_c). The samples were coated under several coating parameters, where the temperature and time of the coating and annealing process were changed. After coating, the surface condition, composition ratio of the tin, Nb_3Sn film thickness, and superconducting temperature,T_c, were evaluated. Surface observation and composition ratio measurements were performed using scanning electron microscopy (SEM) and energy-dispersive X-ray spectroscopy (EDX). The Nb foils were embedded in a resin and polished, and the cross-sections were evaluated using SEM. The T_c of the samples was evaluated by measuring the temperature versus anti magnetization for each applied magnetic field using a magnetic property measurement system. Table 1 shows the typical sample coating result. Figure 2 shows the surface SEM images of the 9th and 23rd sample in Table 1.

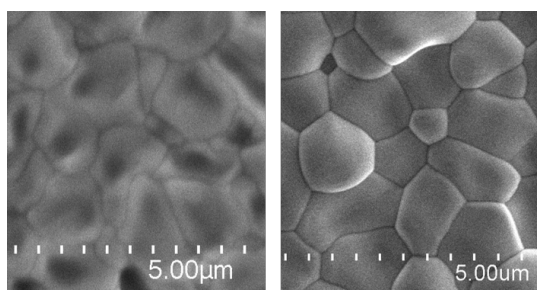

Figure 2: SEM image of the samples' surface. Left: the 9th sample; Right: the 23rd sample.

The T_c and tin composition ratio of the 4th sample were lower than that of the 9th and 23rd samples. The coating temperature of the 4th sample was 1200 °C; therefore, the diffusion rate of tin was faster in this sample than in the others. The tin diffused deep into the Nb substrate of the 4th sample, and consequently, the tin composition ratio on the surface became lower than that in the other sample. The T_c was lower than 18 K when the tin composition ratio was lower than 25 atomic percent (at %). Therefore, the T_c of the 4th sample with a low tin composition ratio was also

* kotaro@post.kek.jp

ISBN: 978-3-95450-233-2 ISSN: 2673-5504 doi:10.18429/JACoW-SRF2021-SUPCAV009

Table 1: Sample Coating Result

Number of coating	2nd	4th	9th	11th	23rd
Coating Time [h]	6.5	1.5	1.5	1.5	3.0
Coating Temperature (Furnace) [°C]	1100	1200	1100	1100	1100
Coating Temperature (Tin heater) [°C]	1300	1400	1400	1400	1400
Annealing Time [h]	1	1.5	1.5	0	0
T_c [K]	16.1±0.1	11.1±0.1	18.0±0.2	17.9±0.4	18.1±0.1
Thickness [µm]	1.7± 0.4	-	1.7±0.2	1.3±0.3	1.5±0.3
Sn at %	22.8	18.2	24.1	23.5	24.0
Voids	☑	☑	☑	none	none

considered to be low. This result was consistent with earlier studies [3]. Patchy regions were observed all sample surface. The surface of the Nb_3Sn grains was concave, and voids were observed in the samples after annealing. The cavity performance degraded with the presence of voids on the cavity surface [4]. The T_c of the 9th and 23rd samples, in which the coating temperature was same, but no annealing process was applied for 23rd sample, was almost the same. However, few voids are observed on the 23rd samples, that was coated without annealing process. The Nb_3Sn coating pattern of the 23rd sample, which had a high T_c value and no voids on the surface, was chosen for the cavity coating.

CAVITY COATING

Nb_3Sn coating for TESLA-like single-cell cavity was performed using the KEK coating system. Figure 3 shows the cavity coating setup. To evaluate the quality of the Nb_3Sn coating, two witness samples were placed inside the cavity. One of the samples was a Nb plate, and the other was a Nb film. Prior to coating the Nb_3Sn, the Nb cavity was electropolished. The cavity surface was polished for approximately 20 µm. The coating system was degassed with the cavity at 120°C for 9 h, and Nb_3Sn coating for the cavity was performed after degassing. The coating parameter for the cavity was the same as that of the 23rd sample. The nucleation process was performed at 500°C for 4.5 h; the coating process was performed at 1100°C for 3 h. The annealing process was omitted. Figure 4 shows the temperature profile and RGA profile during cavity coating. Figure 4 shows that the partial pressure of mass 36(HCl) and mass 71(Cl_2) became higher than the other components' partial pressures when the nucleation process started. It was suggested that these partial pressures originated from the $SnCl_2$ that evaporated during the nucleation process. The partial pressure of mass 18(H_2O) was higher than other components' partial pressures during the Nb_3Sn coating. This result suggests that the degassing process before the Nb_3Sn coating was insufficient to get rid of the water.

Figure 5 shows photographs of the cavity's inner surface before and after Nb_3Sn coating. Both were taken from the perspective. After Nb_3Sn coating, the inner surface of the cavity had a matte finish. The surface was very similar

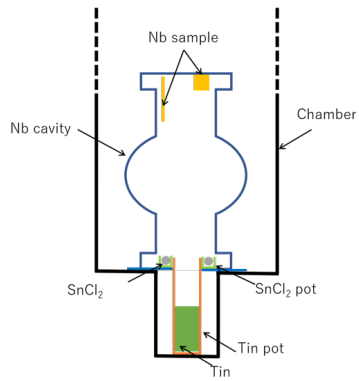

Figure 3: Coating setup for the TESLA-like single-cell cavity. Witness samples were placed inside the cavity to evaluate the quality of the Nb_3Sn coating.

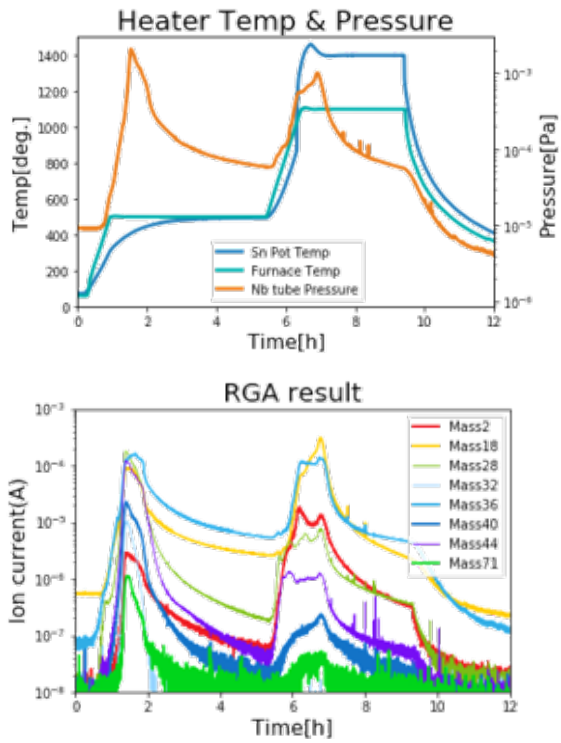

Figure 4: Top: Temperature profile of the cavity coating. In the coating process, the furnace temperature was 1100°C, and the tin heater temperature was 1400°C. Bottom: Partial pressure of the cavity coating.

ISBN: 978-3-95450-233-2 ISSN: 2673-5504 doi:10.18429/JACoW-SRF2021-SUPCAV009

to the coating surface obtained at Cornell University and JLab [5, 6].

Figure 5: Left: Cavity inner surface before coating. Right: Cavity inner surface after coating.

The characteristics of witness samples were determined using SEM/EDX. Figure 6 shows an SEM image of the witness sample surface. The composition ratio of tin on the surface was 23.9 ± 2.0 at %.

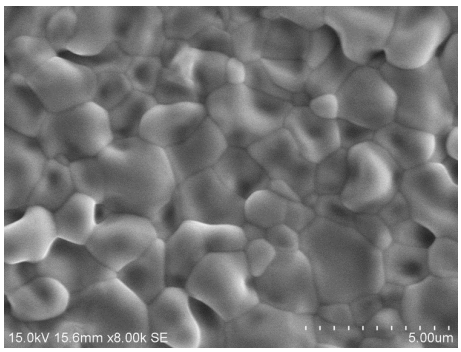

Figure 6: SEM images of the witness samples. The samples were coated with the cavity.

CAVITY PERFORMANCE RESULT

The vertical cavity performance test was conducted after cavity coating. The magnetic flux change was also measured at approximately 18 K. In the performance test, 3 cernox sensors were used to measure the cavity temperature, 40 carbon sensors were used for measuring the cavity heating position, and 8 flux gate sensors were used for measuring the magnetic flux change when the cavity became superconducting. Figure 7 shows a schematic of the sensors' positions, and Fig. 8 shows a photograph of the sensors.

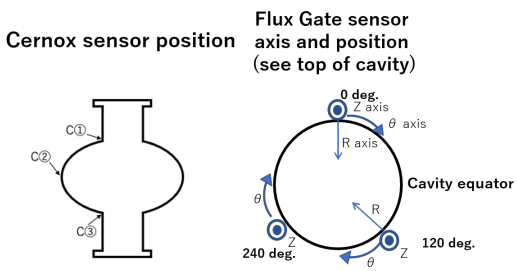

Figure 7: Schematics of the sensors' positions in the vertical cavity test. The left schematic shows the position of the Cernox sensors. Cernox sensors were placed at the top iris, bottom iris, and equator. The right schematic shows the positions of the flux gate sensors. The flux gate sensors were placed at 0°, 120°, and 240°.

The Cernox sensors were located on the top iris, bottom iris, and equator for measuring the cavity temperature, as shown in Fig. 7 (Left). The cavity temperature difference when the Nb_3Sn film became a superconducting state, ΔT, was defined as the temperature difference between the top and bottom irises. The Flux gate sensors were placed at 0°, 120°, and 240°, as shown in Fig. 7 (right). At 0° and 120°, the flux gate sensors were placed in the cavity vertical (Z-axis), cavity equatorial (θ-axis), and cavity radial (R-axis) directions. At 240°, flux gate sensors were placed in the Z-axis and the θ-axis.

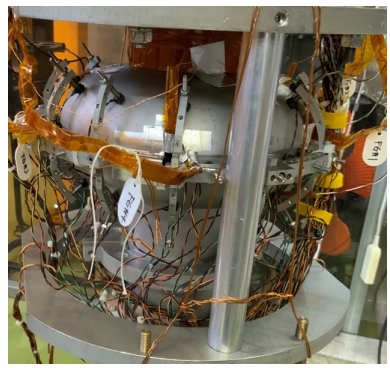

Figure 8: Photograph of the carbon sensors and flux gate sensors.

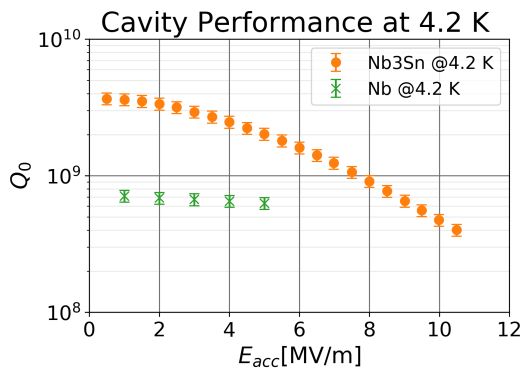

Figure 9: Cavity performance measurement result at 4.2 K. The orange plots show the cavity performance after the Nb_3Sn coating, and the green plots show the cavity performance prior to coating.

The cavity performances were measured at 4.2 K and below 4 K when ΔT was 0.01 K, 0.20 K, 0.23 K, and 1.0 K. Figure 9 shows the cavity performance at 4.2 K. Figure 10 shows the cavity performance below 4.2 K when ΔT was 0.01 K. In Fig. 9, the performance of the Nb_3Sn cavity is plotted when ΔT was 0.01 K.

In Fig. 9, the Q value of the Nb surface was 7.1×10^8 at 4.2 K when E_{acc} was 1 MV/m. In contrast, the Q value after the Nb_3Sn coating was 3.9×10^9 when E_{acc} was 1 MV/m and ΔT was 0.01 K. These results suggest that the surface was successfully coated with Nb_3Sn. In each cavity performance test, the heating points were the cavity equator between 42° and 72° The cavity was quenched when E_{acc} was approximately 11 MV/m.

ISBN: 978-3-95450-233-2 ISSN: 2673-5504 doi:10.18429/JACoW-SRF2021-SUPCAV009

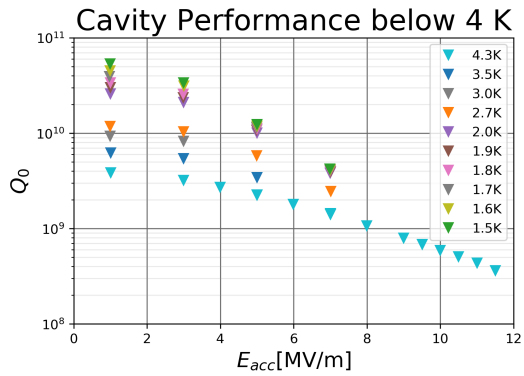

Figure 10: Cavity performance measurement result below 4 K. In this measurement, Δ T was 0.01 K.

The surface resistance was decomposed into BCS resistance (R_{BCS}) and residual resistance (R_{res}) from each Nb_3Sn cavity performance result at each ΔT . Figure 11 shows the ΔT dependence on R_{BCS} and R_{res} in each E_{acc}. The horizontal axis shows ΔT, and the vertical axes shows R_{BCS} and R_{res} in Fig. 11. R_{BCS} was almost constant regardless of ΔT, but R_{res} increased depending on ΔT in each E_{acc}.

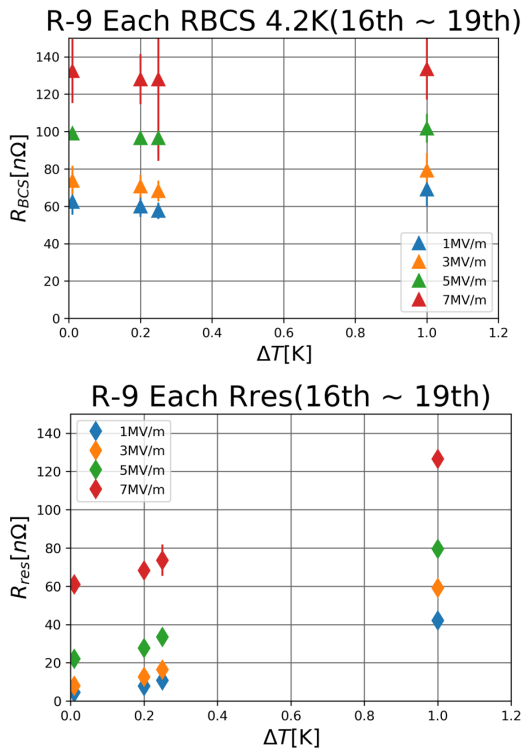

Figure 11: ΔT dependence of R_{BCS}(top) and R_{res}(bottom) in each E_{acc}. The horizontal axis is ΔT, and the vertical axes represent R_{BCS} and R_{res}. R_{res} increased depending on ΔT.

The magnetic flux change was measured when the external magnetic field was 0 mG and ± 50 mG. In the measurement, Δ T was 0 K and 1 K. Figure 12 shows the magnetic field difference between the normal state and superconducting state in the Z-axis, R-axis, and θ-axis. The horizontal axis shows the external magnetic field, and the vertical axis shows the magnetic field difference between the normal and superconducting states. The Z-axis result is displayed in the top of Fig. 12; the R-axis result is displayed in the center of Fig. 12; the θ-axis result is displayed in the bottom of Fig. 12. The circle plots show the magnetic field change when Δ T was 0 K, and the diamond plots show the magnetic field change when Δ T was 1 K. The blue plots show the results at 0°; the orange plots show the results at 120°, and green plots show the results at 240°.

Figure 12 shows that the magnetic field difference was close to zero when ΔT was 0 K, regardless of the external magnetic field. Conversely, the magnetic field changed by several mG when ΔT was 1 K.

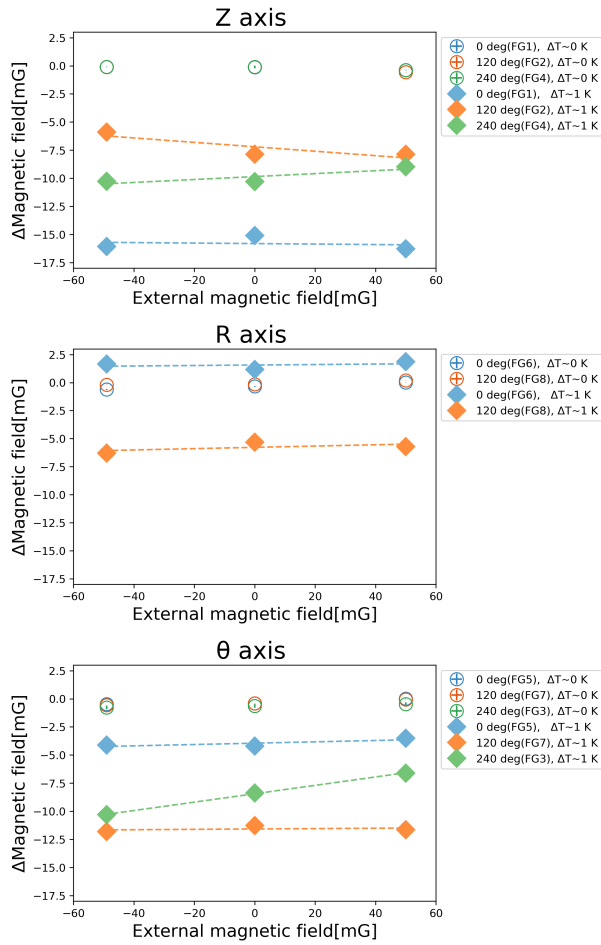

Figure 12: External magnetic field vs magnetic flux change between the normal and superconducting state.

DISCUSSION

The cavity performance was measured after applying the Nb_3Sn coating on the single-cell cavity. In this result, the Q-value of the cavity was less than 1 $\times 10^{10}$ at 4.2 K, as shown in Fig. 9 . The clean booth of the coating system was not yet built when the Nb_3Sn coating was applied to the cavity. Therefore, it is possible that carbon impurities were introduced into the Nb_3Sn film. In addition, an annealing

ISBN: 978-3-95450-233-2 ISSN: 2673-5504 doi:10.18429/JACoW-SRF2021-SUPCAV009

process was omitted in this coating. There is a possibility that Nb-Sn compounds, other than Nb_3Sn, whose T_c value is lower than that of Nb_3Sn were formed without sufficient reaction of tin [3]. Tin is also a superconductor with a T_c of approximately 3.7 K [7]. Superconductors with lower T_c than Nb_3Sn can decrease the superconducting gap and increase the cavity surface resistance [8].

It was reported that the cavity performance degraded with the patchy region on the cavity surface [9]. Since the 23rd sample has patchy region on its surface, the cavity surface coated in this study might also have patchy region. This might degraded the cavity performance.

Figure 11 shows that the R_{BCS} was nearly constant, even as ΔT increased. However, the R_{res} showed large dependence on ΔT. The surface resistance of the Nb_3Sn increased depending on the temperature difference between the top and bottom irises. The results indicate that the R_{res} increased owing to the trapping of the magnetic flux generated by the thermoelectric effect when there is a temperature difference between the irises.

In Fig. 12, the magnetic field change when the cavity temperature was approximately 18 K was close to zero regardless of the external magnetic field when Δ T was 0 K. The magnetic field changed by several mG when ΔT was 1 K in each external magnetic field. In the case of Nb cavities, the magnetic field change at the equator is proportional to the external magnetic field [10–12]. However, the magnetic field changes in the Nb_3Sn cavity did not depend on the external magnetic field in each axis, as shown in Fig. 12. These results suggest that the magnetic field change due to the external magnetic field was not measured from the Nb_3Sn cavity in this measurement. These results also suggest that the magnetic field change in the Nb_3Sn cavity is dominated by the thermo-electric effect.

SUMMARY AND OUTLOOK

After constructing the Nb_3Sn coating system, a Nb_3Sn coating was applied to the samples at KEK. There were voids on the surface when the annealing process was 1.5 h long. However, there were only a few voids on the surface when the annealing process was omitted. The coating parameters for the cavity were determined as follows: The nucleation process was conducted at 500 °C for 3.0 h, the furnace temperature was 1100 °C, and the tin heater temperature was maintained at 1400 °C for 3.0 h during the coating process, and the annealing process was omitted. After determining the coating parameter, a Nb_3Sn coating was applied to the 1.3 GHz single-cell cavity, and the cavity performance was measured. The Q value of the cavity was 3.9×10^{10} at 4.2 K and 1 MV/m. The magnetic field changes at approximately 18 K were investigated, and it was found that the flux change from the thermo-electric effect was dominant.

A clean booth of the coating system was built to prevent impurities in order to realize a high-efficiency Nb_3Sn cavity. Further anodization will be applied for the Nb substrate to reduce abnormal growth during coating. In addition, details of the magnetic field change during the superconducting transition of the Nb_3Sn film will be evaluated.

ACKNOWLEDGMENT

This work was supported by TIA Kakehashi TK20-035. We would like to thank Editage for English language editing.

REFERENCES

[1] K. Takahashi, K. Umemori, T. Konomi, H. Sakai, E. Kako, H. Ito, and T. Okada, "Design and construction of Nb_3Sn vapor diffusion coating system at KEK," presented at SRF2021, 2021, paper SUPCAV008, to be published, this conference.

[2] S. Posen and D. L. Hall, "Nb3sn superconducting radiofrequency cavities: fabrication, results, properties, and prospects," *Superconductor Science and Technology*, vol. 30, no. 3, p. 033004, 2017.

[3] A. Godeke, "A review of the properties of nb3sn and their variation with a15 composition, morphology and strain state," *Superconductor Science and Technology*, vol. 19, no. 8, p. R68, 2006.

[4] Z. Yang, H. Guo, Y. He, C. Li, Z. Lin, M. Lu, T. Tan, P. Xiong, S. Zhang, and S. Zhang, "Development of Nb_3Sn Cavity Coating at IMP," in *Proc. SRF'19*, Dresden, Germany, Jun.-Jul. 2019, pp. 21–24. doi:10.18429/JACoW-SRF2019-MOP003

[5] S. Posen and M. Liepe, "Advances in development of nb_3Sn superconducting radio-frequency cavities," *Phys. Rev. ST Accel. Beams*, vol. 17, p. 112001, Nov 2014.

[6] U. Pudasaini, G. Eremeev, C. E. Reece, J. Tuggle, and M. J. Kelley, "Analysis of RF losses and material characterization of samples removed from a nb3sn-coated superconducting RF cavity," *Superconductor Science and Technology*, vol. 33, no. 4, p. 045012, feb 2020.

[7] W. De Haas, J. De Boer, and G. Van den Berg, "The electrical resistance of cadmium, thallium and tin at low temperatures," *Physica*, vol. 2, no. 1, pp. 453 – 459, 1935.

[8] T. Kubo and A. Gurevich, "Field-dependent nonlinear surface resistance and its optimization by surface nanostructuring in superconductors," *Phys. Rev. B*, vol. 100, p. 064522, Aug 2019.

[9] D. Hall, J. Kaufman, M. Liepe, R. Porter, and J. Sears, "First Results From New Single-Cell Nb_3Sn Cavities Coated at Cornell University," in *Proc. 8th Int. Particle Accelerator Conf. (IPAC'17)*, Copenhagen, Denmark, May 2017, pp. 40–43. https://doi.org/10.18429/JACoW-IPAC2017-MOOCA2

[10] A. Romanenko, A. Grassellino, D. Crawford, A.C.and Sergatskov, and O. Melnychuk, "Ultra-high quality factors in superconducting niobium cavities in ambient magnetic fields up to 190 mg," *Applied Physics Letters*, vol. 105, no. 23, p. 234103, 2014.

[11] S. Posen, M. Checchin, A. C. Crawford, A. Grassellino, M. Martinello, O. S. Melnychuk, A. Romanenko, D. A. Sergatskov, and Y. Trenikhina, "Efficient expulsion of magnetic flux in superconducting radiofrequency cavities for high q 0 applications," *Journal of Applied Physics*, vol. 119, no. 21, p. 213903, 2016.

[12] "Flux expulsion experiments at KEK," TTC 2018.